Research Article

Atomic-Level Investigation of CH_x and C_2H_x Adsorption on β-SiC (111) Surface for CVD Diamond Growth from DFT Calculations

Naichao Chen and Fanghong Sun

School of Mechanical Engineering, Shanghai Jiao Tong University, Shanghai 200240, China

Correspondence should be addressed to Fanghong Sun, sunfanghong@sjtu.edu.cn

The focus of this paper is on the adsorption of unsaturated hydrocarbon molecules on β-SiC (111) surfaces during diamond film growth. The CH_x and C_2H_x molecules have been investigated to obtain a specific insight into absorbing diamond processes on the atomic scale. Structural and electronic properties of CH_x and C_2H_x adsorption on the Si- and C-terminated surfaces have been studied by first-principles calculations based on density functional theory (DFT). From the calculated energetics and geometries, we find that C_2H_x adsorption on the Si-terminated surfaces has six possible surface reconstructions. For the C-terminated surface, there exist eight possible surface reconstructions. Five surface reconstructions, including CH_2 adsorption on the Si- and C-terminated surface, $CH–CH_2$ and $CH=CH_2$ adsorption on the C-terminated surface, and C_2H_5 adsorption on the Si-terminated surface, have the largest hydrogen adsorption energies and more stability of surface reconstructions. Calculations demonstrate that the Si-terminated surface is energetically more favorable for fabricating CVD diamond coatings than the C-terminated surface.

1. Introduction

A variety of chemical vapor deposition (CVD) techniques are able to deposit diamond films [1–3]. The intrinsic reactivity of a hetero-substrate under CVD plasma strongly determines the mechanisms competing with diamond nucleation. These mechanisms have often detrimental consequences on the quality of the interface with diamond [4, 5]. The chemical kinetic model of CVD has been developed to study the detailed descriptions of both gas-phase and surface processes occurring in gas-activated deposition of diamond film [2, 3, 6]. Several reaction pathways describing deposition of diamond initiated by different gaseous species, including the CH_3, C_2H_2, C [3], and several C_2H_x [6] species, have provided a specific insight into chemical processes. These techniques are capable of identifying the activation of the growing surface. In addition, the theoretical model has been employed to investigate diamond formation by combining mass, momentum, and energy balance equations for the gas flow with detailed chemical mechanisms for the gas phase and surface chemistry [2, 7]. The gas phase composition profile and surface chemical kinetics for diamond formation have been solved. However, these types of issues do not well

and enough describe the growth mechanism of diamond film and the acquiring diamond film of high quality efficiently. The surface diffusion [1] and quantum-mechanical calculations and localized kinetic analysis [8] farther highlight an understanding of the atomic-scale dynamics that lead to the CVD of diamond formation.

Recently, the CVD diamond coatings on SiC substrates have been investigated [5, 9, 10]. The formation of carbon phase and the roughening of the 3C–SiC surface have been observed [4]. Therefore, adsorption of unsaturated hydrocarbon molecules on SiC surfaces is of great importance to investigate the initial-stage growth of diamond film on SiC substrates. At the same time, the SiC surface and its reconstructions have attracted much attention both in experiment [11] and theory [12] due to its fundamental interest and technological importance in recent years. Progresses in several theoretical applications, such as *ab initio* [13, 14] and empirical molecular dynamic [15, 16], have provided more specific insight into absorbing processes on the atomic scale. The surface relaxation and reconstructing behaviors have been derived from these calculations. The chemisorption of C_2H_2 and CH_3 molecules onto the silicon carbide terminated (2×1) surface suggests that optimal C_2H_2

chemisorption has been found to occur with the adsorbate molecule situated above the cave site, while optimal CH_3 chemisorption has been observed to present with the CH_3 radicals bonding directly to the surface dangling bonds [17]. Structural and electronic properties of acetylene and ethylene adsorbed on β-SiC (001) surface with dimer site have been investigated based on density functional theory [18, 19]. However, the mechanism underlying diamond deposition [1, 6] has suggested that the carbon-carbon bond oriented in a direction parallel to the dimer site has not always occurred in the progress of the CVD diamond film growth. Up to now, the mechanisms of the CVD diamond formation on β-SiC surfaces have been seldom studied.

This state of the art has motivated the present study. The purpose of present work is to concentrate on the adsorption of hydrocarbons on the β-SiC (111) surface. Obviously, the growth species cannot be limited to only acetylene and ethylene in the process of CVD diamond film growth. In this paper, the CH_x and C_2H_x adsorption on the β-SiC (111) surface has been studied by first-principles pseudopotential plane-wave method within the density functional theory (DFT). The geometry optimization has provided the surface relaxation and configuration. In addition, all the total energies of the surface reconstructions have been calculated to obtain structural properties. Thus, our computational results could promote the proper understanding on the growth mechanism of CVD diamond film on the β-SiC (111) surface.

2. Theoretical Model

Various complex prototypes occurred on the β-SiC (111) substrate surface are very hard to ascertain [20]. Therefore, the substrate surface in this work is assumed as the ideal β-SiC (111) structure in order to reduce the complexity. Although this study focused on these simple cases, the atomic-level investigation might be useful for understanding the real processors in the growth mechanism of CVD diamond film on the β-SiC (111) surface.

In order to account for per molecular adsorption on the β-SiC (111) substrate surface, the study is first made of determining the covalently bonds to CH_x and C_2H_x gaseous species. The chemical reaction mechanism described by the chemical kinetics of diamond deposition [6] showed the conversion of CH_x and C_2H_x gaseous species into the surface species. The models have been designed to be as many as possible. In this paper, all the structural and electronic properties of CH_x and C_2H_x gaseous species adsorbed on the β-SiC (111) substrate surface have been studied. Namely, the CH_x gaseous species includes the C, CH CH_2, and CH_3 molecules; the C_2H_x gaseous species includes the $C_2, C_2H, C_2H_2, C_2H_3, C_2H_4$, and C_2H_5 molecules. The detailed analysis of making these models is presented in following parts.

Geometry optimizations, especially the movement of unsaturated hydrocarbon atoms, have been firstly studied to contribute to a fundamental understanding of surface reconstructions by the chemistry of hydrocarbons on the β-SiC (111) surfaces, which is of crucial technological importance.

TABLE 1: The surface reactions on the β-SiC (111) surface.

No.	Si-terminated surface reactions	C-terminated surface reactions
1	$Si_{d(s)}+H_{(g)} \leftrightarrow Si_d–H(s)$	$C_{d(s)}+H_{(g)} \leftrightarrow C_d–H(s)$
2	$Si_{d(s)}+C_{(g)} \leftrightarrow Si_d–C(s)$	$C_{d(s)}+C_{(g)} \leftrightarrow C_d–C(s)$
3	$Si_{d(s)}+CH_{(g)} \leftrightarrow Si_d–CH(s)$	$C_{d(s)}+CH_{(g)} \leftrightarrow C_d–CH(s)$
4	$Si_{d(s)}+CH_{2(g)} \leftrightarrow Si_d–CH_2(s)$	$C_{d(s)}+CH_{2(g)} \leftrightarrow C_d–CH_{2(s)}$
5	$Si_{d(s)}+CH_{3(g)} \leftrightarrow Si_d–CH_3(s)$	$C_{d(s)}+CH_{3(g)} \leftrightarrow C_d–CH_{3(s)}$
6	$Si_{d(s)}+C_{2(g)} \leftrightarrow Si_d–C_2(s)$	$C_{d(s)}+C_{2(g)} \leftrightarrow C_d–C_2(s)$
7	$Si_{d(s)}+C_2H_{(g)} \leftrightarrow Si_d–C_2H(s)$	$C_{d(s)}+C_2H_{(g)} \leftrightarrow C_d–C_2H(s)$
8	$Si_{d(s)}+C_2H_{2(g)} \leftrightarrow Si_d–C_2H_2(s)$	$C_{d(s)}+C_2H_{2(g)} \leftrightarrow C_d–C_2H_2(s)$
9	$Si_{d(s)}+ C_2H_{3(g)} \leftrightarrow Si_d–C_2H_3(s)$	$C_{d(s)}+C_2H_{3(g)} \leftrightarrow C_d–C_2H_3(s)$
10	$Si_{d(s)}+ C_2H_{4(g)} \leftrightarrow Si_d–C_2H_4(s)$	$C_{d(s)}+C_2H_{4(g)} \leftrightarrow C_d–C_2H_4(s)$
11	$Si_{d(s)}+C_2H_{5(g)} \leftrightarrow Si_d–C_2H_5(s)$	$C_{d(s)}+C_2H_{5(g)} \leftrightarrow C_d–C_2H_5(s)$

TABLE 2: The nomenclature of the structures of C_2H_x adsorption.

Name used	Structure	
	Si-terminated surface	C-terminated surface
$X_d–C_2H(I)$	$Si_d–C–CH$	$C_d–C–CH$
$X_d–C_2H(II)$	$Si_d–CH–C$	$C_d–CH–C$
$X_d–C_2H_2(I)$	$Si_d–C–CH_2$	$C_d–C–CH_2$
$X_d–C_2H_2(II)$	$Si_d–CH_2–C$	$C_d–CH_2–C$
$X_d–C_2H_2(III)$	$Si_d–CH–CH$	$C_d–CH–CH$
$X_d–C_2H_2(IV)$	$Si_d–C=CH_2$	$C_d–C=CH_2$
$X_d–C_2H_2(V)$	$Si_d–CH=CH$	$C_d–CH=CH$
$X_d–C_2H_3(I)$	$Si_d–C–CH_3$	$C_d–C–CH_3$
$X_d–C_2H_3(II)$	$Si_d–CH–CH_2$	$C_d–CH–CH_2$
$X_d–C_2H_3(III)$	$Si_d–CH_2–CH$	$C_d–CH_3–CH$
$X_d–C_2H_3(IV)$	$Si_d–CH=CH_2$	$C_d–CH=CH_2$
$X_d–C_2H_4(I)$	$Si_d–CH–CH_3$	$C_d–CH–CH_3$
$X_d–C_2H_4(II)$	$Si_d–CH_2–CH_2$	$C_d–CH_2–CH_2$
$X_d–C_2H_5$	$Si_d–CH_2–CH_3$	$C_d–CH_2–CH_3$

The associated energy variation of the species adsorbed on the surface has terminally provided the structural and electronic reconstructions. It is well known that the most stable structure always has the minimum energy among the structures with atoms of the same element. In order to obtain the feasible surface reconstructions, the total energies of the CH_x and C_2H_x adsorption on the β-SiC (111) surface have been calculated by DFT method. The two substrate surfaces [20], Si- and C-terminated surfaces, have been developed to investigate different SiC surfaces in this work. The associated chemical reaction model is provided in Table 1.

The surface sites are defined as follows. "X_d" represents a radical site; "X_dR" represents an "R" bonded to "X_d" radical. "X" denotes Si or C atom; "R" denotes CH_n ($n = 0, 1, 2, 3$) or C_2H_m ($m = 0, 1, 2, 3, 4, 5$). The subscript s in each chemical reactor represents the surface site, and g means the vapor gas. In order to distinguish the CH_x and C_2H_x adsorption on the Si- or C-terminated surface, the symbols are employed to represent the associated surface reconstructions. The nomenclatures are given in Table 2.

TABLE 3: The difference in total energy between C adsorption and the other CH_x adsorption on Si- and C-terminated surfaces.

Species	Si-terminated surface (eV)	C-terminated surface (eV)
CH	−17.9042	−17.0661
CH_2	−35.4609	−34.5021
CH_3	−52.3329	−51.4378

The calculations have been carried out by the DFT method which implemented in the simulation tool of DMol^3 [21–23]. The surface has been modeled as a slab using only one β-SiC (111) unit cell for simplifying the structures and concentrating on the effectiveness of the CH_x and C_2H_x adsorption on the β-SiC (111) surface. The slab consisted of two crystal lattices with four layers, and the bottom dangling bonds layers are saturated by hydrogen atoms. The slab is separated from the neighboring slab in the (111) direction by 10 Å of vacuum thickness. The Monkhorst-Pack [24] scheme with $8 \times 8 \times 2$ k-point mesh has been employed for the Brillouin zone integration and geometry optimization.

3. Results and Discussions

The total energies of the surface reconstructions in this work refer to the energy of a specific arrangement of atoms based on the equations of quantum mechanics. The zero of energy is taken to be the infinite separation of all electrons and nuclei. Total energy is generally negative, corresponding to a bound state. In addition, total energy reflects the well-known fact that the most stable surface reconstruction only has the minimum total energy.

The total energies of all CH_x and C_2H_x species adsorbed on activated sites are shown in Figure 1 (where DB is dangling bond). The periodic models of Si-terminated surface behave very similarly to C-terminated surface. The results indicate that the difference between Si- and C-terminated surfaces is small in comparison. There are clearly some significant variations in the calculated reconstruction energies (and hence in the predicted minimum energy structures) that must be mentioned (Figure 1(c)). As can be seen by comparing the values for the various structural models, the maxima correspond to the C_2H_2 (II) species, and the difference is less than 0.1 hartree.

The computational results reveal that the silicon or carbon atom saturated by hydrogen atoms on the top layer surface is the most effective in increasing the stabilities of CH_x and C_2H_x adsorption on the β-SiC (111) surface by comparing surface with dangling bond. This is in good agreement with earlier surface studies [25]. The associated values suggest that the CH_3 radical molecule could form the most stable surface reconstruction among the CH_x adsorptions on the β-SiC (111) surface, which is consistent with the results of theoretical calculations [26]. The value of difference in Table 3 indicates that the hydrogen adsorption energy of C species adsorbed on the Si-terminated surface is a more attractive possibility than that of the C adsorption on the C-terminated surface. The difference in total energy between them has reached as high as 0.838 eV per (1×1) unit
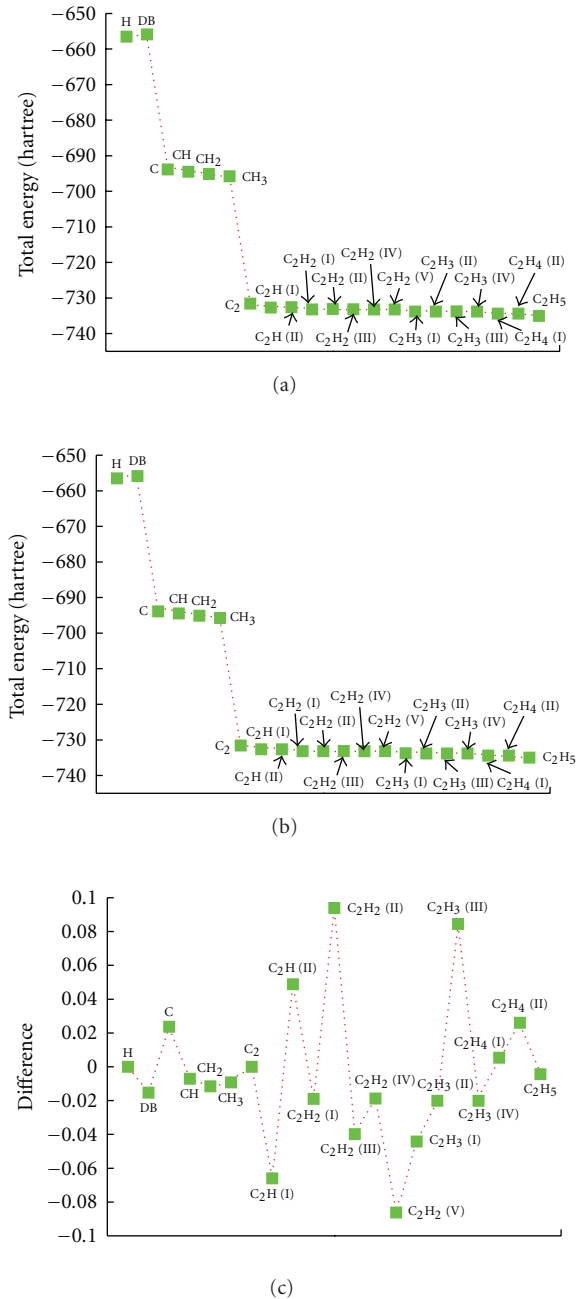

FIGURE 1: Total energies of CH_x and C_2H_x adsorption on the β-SiC (111) surface. (a) Total energies of CH_x and C_2H_x adsorption on the Si-terminated surface, (b) total energies of CH_x and C_2H_x adsorption on the C-terminated surface, and (c) the difference in total energies of CH_x and C_2H_x adsorption between Si- and C-terminated surfaces.

cell. At the same time, the CH_2 species has greater relevant step towards the formation of adsorbing the hydrogen by comparison with the CH species. The corresponding difference is 0.500 and 0.682 eV, respectively. These results agree with the previous theoretical studies very closely [27]. The calculated values of total energies suggest that the Si-terminated surface is easier to adsorb the CH_x molecules than the C-terminated surface.

Table 4: The difference in total energy between C_2 adsorption and the other C_2H_x adsorption on Si- and C-terminated surfaces.

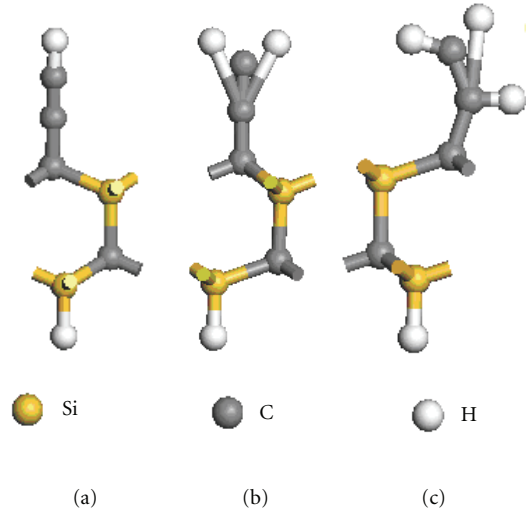| Species	Si-terminated surface (eV)	C-terminated surface (eV)
C_2H (I)	-29.8228	-28.0097
C_2H (II)	-26.6949	-28.0061
C_2H_2(I)	-44.2762	-43.7435
C_2H_2 (II)	-41.2048	-43.7434
C_2H_2 (III)	-43.3547	-42.253
C_2H_2 (IV)	-44.2761	-43.7485
C_2H_2 (V)	-44.974	-42.6138
C_2H_3 (I)	-60.3894	-59.1696
C_2H_3 (II)	-61.1584	-60.5944
C_2H_3 (III)	-58.3127	-60.5957
C_2H_3 (IV)	-61.158	-60.5945
C_2H_4 (I)	-76.5272	-76.6586
C_2H_4 (II)	-75.967	-76.6585
C_2H_5	-93.4121	-93.2752

Figure 2: The optimizing geometry of C_2H_x adsorption on the C-terminated surface: (a) the CH–C adsorption, (b) the CH$_2$–C adsorption, and (c) the CH$_2$–CH adsorption.

However, the C_2H_x species is complex as various prototypes can exist under certain conditions, including C–C and C=C bond. In this paper, all of the C_2H_x allotropes are studied in theory by DFT method to obtain the structural properties (see Table 4). Our results reveal that the C_2H (I) adsorption on the Si-terminated surface is slightly favored with respect to the C-terminated surface. Interestingly, total energies of C_2H (I) and C_2H (II) species adsorbed on C-terminated surface remain slightly the same, which indicates that the relative position of the intramolecular hydrogen bond has small influences on the stability of the surface reconstruction. The calculated results based on the analysis of total energies suggest that these two surface reconstructions will occur at the same time during the CVD diamond formation. Figure 2(a) shows the optimized structure model for C_2H (II) adsorption, where the adsorbed molecule has a C–H bond length of 2.27 Å. As far as the energetics and the geometries are concerned, we confirm that the C_2H (II) adsorption on C-terminated surface cannot present in the process of CVD diamond film growth.

Five allotropes of C_2H_2 species are investigated in this paper. As can be seen the C_2H_2 (I) adsorption holds the most stability of surface reconstruction among the five allotropes. By comparison of the total energies of C_2H_2 (I) and C_2H_2 (II) adsorption, it is no surprise to find that these two surface reconstructions have the same probability occurring during diamond formation, while the C–H bond length of 2.10 Å indicates that the C_2H_2 (II) adsorption does not occur in practical CVD diamond coating (see Figure 2(b)). Interestingly, the geometry optimization shows that the C_2H_2(II) adsorption can terminally migrate to C_2H_2 (I) adsorption. Consequently, C_2H_2 (I) species is energetically more favorable for fabricating CVD diamond coatings than C_2H_2(II) species. Due to the large total energy, the C_2H_2(II) adsorption is hard to form the surface reconstruction in situ.

For C_2H_2(IV) and C_2H_2(V) species with a C=C bond, the C_2H_2(IV) adsorption on the C-terminated surface is slightly favored with respect to C_2H_2(V) adsorption. Conversely, the C_2H_2(V) adsorption on the Si-terminated surface is found to be the most effective in the stability of surface reconstruction. In addition, from the calculated adsorption energies, the species with a C=C bond are energetically more favorable for fabricating CVD diamond coatings than those with a C–C bond. This conclusion is evident by looking at the result of kinetic Monte Carlo (KMC) simulations [1].

Similarly, the C_2H_3 adsorption on the β-SiC (111) surface has four surface reconstructions. For the Si-terminated surface, the calculated results reveal that the C_2H_3 (II) and C_2H_3 (IV) adsorption has the most favorable stability of surface reconstructions. It is worth noting that more hydrogen atoms saturating the top layer species, such as C–CH$_3$ adsorption, will result in more stability of the surface reconstructions. Additionally, the simulations also find very similar values for Si$_d$–CH–CH$_2$ and Si$_d$–CH=CH$_2$ surface reconstructions. This is consistent with the adsorbing activity of Si$_d$–C–CH2 and Si$_d$–C=CH$_2$ surface reconstructions, while this state differs significantly for both Si$_d$–CH–CH surface reconstruction and Si$_d$–CH=CH surface reconstruction. Obviously, the carbon-carbon single or double bonds do not play a valid role in determining the stability of surface reconstructions. For the C-terminated surface, C_2H_3 (III) adsorption holds the most stability of surface reconstruction. From the calculated geometry, the length of C–H bond is 2.08 Å (see Figure 2(c)), which suggests that C_2H_3 (III) adsorption does not exit during CVD diamond formation. Therefore, C_2H_3 (II) species and C_2H_3 (IV) species are considered as the most stability of surface reconstruction among the C_2H_3 adsorption on the C-terminated surface. Thus, the C_2H_3 (II) and C_2H_3 (IV) adsorption can present at the same time during the diamond film growth.

For the C_2H_4 adsorption, two surface reconstructions are investigated. The calculated results find that C_2H_4 (I) adsorption on the Si-terminated surface has more stability than that of the C_2H_4 (II), while the C_2H_4 (I) adsorption on the C-terminated surface has the same probability with respect to C_2H_4 (II) adsorption. C_2H_5 adsorption on the β-SiC (111) surface has only one surface reconstruction, where both two carbon atoms are saturated by hydrogen atoms.

Therefore, from the energetics and the geometry, we find that the position of hydrogen atoms on the C_2H_x species is the most effective among the stabilities of surface reconstructions. For the C-terminated surface, the surface reconstruction with the saturated carbon atoms on the top layer species is slightly favorable stability with respect to those with dangling bond. However, for the Si-terminated surface, the saturated carbon atom on the sublayer species is useful for the stability of surface reconstructions. Meanwhile, C–CH adsorption on Si- or C-terminated surface has more stability than the C–C adsorption with fully dangling bond. In addition, C_2H_5 adsorption on the C-terminated surface can be formed concurrently at different surface locations through many instances of reactions, such as adsorbing one hydrogen atoms on C_2H_4 species. The calculated values indicate that the C_2H_4 species has larger hydrogen adsorption energy than the others. Therefore, C_2H_5 adsorption has the most favorable stability of surface reconstruction. For the Si-terminated surface, the CH–CH_2 and CH=CH_2 species hold the highest hydrogen adsorption energy, which make these two species more stable. Interestingly, the Si- and C-terminated surfaces do not present the similar properties of adsorbing the CH_x and C_2H_x molecules. The calculated results demonstrate that the Si-terminated surface is much easier to deposit the diamond film than the C-terminated surface.

4. Conclusions

In this paper, the CH_x and C_2H_x adsorption on the β-SiC (111) surface has been investigated to highlight specific insight into the initial-stage growth of diamond film on SiC substrates. The geometry optimization and energies of all the surface reconstructions have been calculated by the DFT method. The calculation of the energetics and the geometry shows that C_2H_x adsorption on the Si-terminated surfaces has six possible surface reconstructions, including C–CH, CH=CH, CH–CH_2, CH=CH_2, CH–CH_3, and CH_2–CH_3 species. The CH–CH_2 and CH=CH_2 species hold the largest hydrogen adsorption energy. For the C-terminated surface, there exist eight possible surface reconstructions which include C–CH, C–CH_2, C=CH_2, CH–CH_2, CH=CH_2, CH–CH_3, CH_2–CH_2, and CH_2–CH_3 species. The hydrogen adsorption energies indicate that C_2H_5 adsorption has the most stability of surface reconstruction. Meanwhile, the CH_2 adsorption on the Si- or C-terminated surface also has the largest hydrogen adsorption energy. Calculations also indicate that position of hydrogen atoms on the C_2H_x species is related to the stabilities of surface reconstructions. The calculated results demonstrate that the Si-terminated surface is energetically more favorable for fabricating CVD diamond coatings than the C-terminated surface.

References

[1] A. Netto and M. Frenklach, "Kinetic Monte Carlo simulations of CVD diamond growth-Interlay among growth, etching, and migration," *Diamond and Related Materials*, vol. 14, no. 10, pp. 1630–1646, 2005.

[2] D. E. Kassmann and T. A. Badgwell, "Analysis of process modifications for efficient diamond chemical vapor deposition," *Diamond and Related Materials*, vol. 5, no. 9, pp. 895–906, 1996.

[3] M. E. Coltrin and D. S. Dandy, "Analysis of diamond growth in subatmospheric dc plasma-gun reactors," *Journal of Applied Physics*, vol. 74, no. 9, pp. 5803–5820, 1993.

[4] J. C. Arnault, S. Saada, S. Delclos et al., "In situ study of the initial stages of diamond deposition on 3C-SiC (100) surfaces: towards the mechanisms of diamond nucleation," *Diamond and Related Materials*, vol. 16, no. 4–7, pp. 690–694, 2007.

[5] S. Chowdhury, E. de Barra, and M. T. Laugier, "Study of mechanical properties of CVD diamond on SiC substrates," *Diamond and Related Materials*, vol. 13, no. 9, pp. 1625–1631, 2004.

[6] M. Frenklach and H. Wang, "Detailed surface and gas-phase chemical kinetics of diamond deposition," *Physical Review B*, vol. 43, no. 2, pp. 1520–1545, 1991.

[7] D. E. Kassmann and T. A. Badgwell, "Modeling diamond chemical vapor deposition in a rotating disk reactor," *Diamond and Related Materials*, vol. 5, no. 3–5, pp. 221–225, 1996.

[8] X. An, G. Liu, F. Wang, and S. Liu, "Electronic structure study of growth species adsorption and reaction on cluster models for the diamond surface using LDA method," *Diamond and Related Materials*, vol. 12, no. 12, pp. 2169–2174, 2003.

[9] S. Chowdhury, E. de Barra, and M. T. Laugier, "Hardness measurement of CVD diamond coatings on SiC substrates," *Surface and Coatings Technology*, vol. 193, no. 1–3, pp. 200–205, 2005.

[10] S. Chowdhury, M. T. Laugier, and J. Henry, "XRD stress analysis of CVD diamond coatings on SiC substrates," *International Journal of Refractory Metals and Hard Materials*, vol. 25, no. 1, pp. 39–45, 2007.

[11] B. Stankiewicz and L. Jurczyszyn, "Computations of STM images of SiC(0 0 1)-c(2 × 2) surface," *Surface Science*, vol. 507–510, pp. 463–467, 2002.

[12] W. Lu, P. Krüger, and J. Pollmann, "Atomic and electronic structure of β-SiC(001)-(3 × 2)," *Physical Review B*, vol. 60, no. 4, pp. 2495–2504, 1999.

[13] A. M. Mazzone, "Acetylene adsorption on Si(1 0 0): a study of the role of surface steps," *Surface Science*, vol. 601, no. 1, pp. 218–226, 2007.

[14] W. Lu, P. Krüger, and J. Pollmann, "Ab initio studies on the β-SiC(001)-(5 × 2) surface," *Physical Review B*, vol. 61, no. 4, pp. 2680–2687, 2000.

[15] C. Koitzsch, D. Conrad, K. Scheerschmidt, and U. Gösele, "Empirical molecular dynamic study of SiC(0001) surface reconstructions and bonded interfaces," *Journal of Applied Physics*, vol. 88, no. 12, pp. 7104–7109, 2000.

[16] M. Schaible, "Empirical molecular dynamics modeling of silicon and silicon dioxide: a review," *Critical Reviews in Solid State and Materials Sciences*, vol. 24, no. 4, pp. 265–323, 1999.

[17] A. J. Dyson and P. V. Smith, "Empirical potential study of the chemisorption of C_2H_2 and CH_3 on the β-SiC(001) surface," *Surface Science*, vol. 396, no. 1–3, pp. 24–39, 1998.

[18] J. Wieferink, P. Krüger, and J. Pollmann, "First-principles study of acetylene adsorption on β-SiC (001)-(3×2)," *Physical Review B*, vol. 75, no. 15, Article ID 153305, 2007.

[19] J. Wieferink, P. Krüger, and J. Pollmann, "First-principles study of acetylene and ethylene adsorption on β-SiC(001)-(2×1)," *Physical Review B*, vol. 73, no. 11, Article ID 115309, 12 pages, 2006.

[20] J. Pollmann, P. Krüger, and M. Sabisch, "Atomic and electronic structure of SiC surfaces from ab-initio calculations," *Physica Status Solidi B*, vol. 202, no. 1, pp. 421–445, 1997.

[21] B. Delley, "An all-electron numerical method for solving the local density functional for polyatomic molecules," *The Journal of Chemical Physics*, vol. 92, no. 1, pp. 508–517, 1990.

[22] B. Delley, "Fast calculation of electrostatics in crystals and large molecules," *Journal of Physical Chemistry*, vol. 100, no. 15, pp. 6107–6110, 1996.

[23] B. Delley, "From molecules to solids with the DMol^3 approach," *Journal of Chemical Physics*, vol. 113, no. 18, pp. 7756–7764, 2000.

[24] H. J. Monkhorst and J. D. Pack, "Special points for Brillouin-zone integrations," *Physical Review B*, vol. 13, no. 12, pp. 5188–5192, 1976.

[25] S. J. Harris, "Mechanism for diamond growth from methyl radicals," *Applied Physics Letters*, vol. 56, no. 23, pp. 2298–2300, 1990.

[26] A. J. Dyson and P. V. Smith, "A molecular dynamics study of the chemisorption of C_2H_2 and CH_3 on the Si(001)-(2×1) surface," *Surface Science*, vol. 375, no. 1, pp. 45–54, 1997.

[27] Y. A. Mankelevich and P. W. May, "New insights into the mechanism of CVD diamond growth: single crystal diamond in MW PECVD reactors," *Diamond and Related Materials*, vol. 17, no. 7–10, pp. 1021–1028, 2008.